Mobile Edge Computing-based Vehicular Cloud of Cooperative Adaptive Driving for Platooning Autonomous Self Driving

Ren-Hung Huang[1], Ben-Jye Chang[2], Yueh-Lin Tsai[2], and Ying-Hsin Liang[3]

***Abstract*—The Cooperative Adaptive Cruise Control (CACC) for Human and Autonomous Self-Driving aims to achieve active safe driving that avoids vehicle accidents or traffic jam by exchanging the road traffic information (e.g., traffic flow, traffic density, velocity variation, etc.) among neighbor vehicles. However, in CACC, the butterfly effect is happened while exhibiting asynchronous brakes that easily lead to backward shockwaves and difficult to be removed. Several critical issues should be addressed in CACC, including: 1) difficult to adaptively control the inter-vehicle distances among neighbor vehicles and the vehicle speed, 2) suffering from the butterfly effect, 3) unstable vehicle traffic flow, etc. For addressing above issues in CACC, this paper proposes the Mobile Edge Computing-based vehicular cloud of Cooperative Adaptive Driving (CAD) approach to avoid shockwaves efficiently in platoon driving. Numerical results demonstrate that CAD approach outperforms the compared approaches in number of shockwaves, average vehicle velocity, and average travel time. Additionally, the adaptive platoon length is determined according to the traffic information gathered from the global and local clouds.**

***Keywords*—MEC, Active safe driving, cooperative platoon driving, shockwave, butterfly effect, CACC, VANETs**

I. Introduction

THIS section first briefly describes the Cooperative active safe driving [1] for achieving active safe driving, and then depicts the Adaptive Cruise Control (ACC) and the Cooperative Adaptive Cruise Control (CACC). Furthermore, we classify the critical issues into two types and the related studies are depicted below.

1.1 Introduction to Active Safe Driving, CACC, Mobile Edge Computing

In [1], extended from ITS [2], adopts VANET [3]-[6] using wireless networking: IEEE 802.11p[3][4] or LTE-V [5][6], as the information sharing network for gathering the information of vehicular traffic and road situation, and then Cooperative-ITS (C-ITS) enables the cooperative mechanism for achieving active safe driving. Several driver-assist mechanisms: Advanced Driver-Assistance Systems (ADAS) [7], ACC [8][9], and CACC [10][11] are proposed to assist driver by using various types of sensors (e.g., radar, image scanner, video detector, etc.) to alarm drivers or to directly involves assistant driving control while having explicit and implicit dangers. However, they suffer from suddenly braking and unstable driving. The asynchronous braking and the stop-and-go results of the precedence vehicles easily yield a significant impact on the driving speed of successor vehicles. The phenomenon is called the butterfly effect [12] that transfers a backward shockwave on the behind vehicle flow and may yield dangers.

In the distributedly assistant driving control (e.g., CACC), several critical issues should be addressed to achieve the safely active safe driving, including 1) a stable safe time headway, 2) a stable car-following distance or a stable inter-vehicle distance, 3) the minimum and maximum driving speeds of different-class of roads, etc.

The related works of the assistant driving control can be classified into two types: 1) cooperative warning and maneuvering [13]-[17] and 2) traffic flow stability and shockwave analysis [18]-[22].

Furthermore, recently, the Mobile Edge Computing (namely MEC) mechanism [23]-[25] is specified to minimize the transmission delay by moving the computing-intensive and data-intensive virtual machine instances of the global cloud to the local site that is near to users. Extensively, the MEC mechanism can be combined and cooperated with the Vehicular Cloud.

1.2. Critical issues, motivations, and objectives of this paper

From related works of cooperative driving control, several critical issues exhibit in CACC for active safe driving. The below issues need be addressed effectively before achieving an efficient cooperative control for active safe driving.

1) In CACC, several works neglect the transmission delay of each wireless link on the packet routing path, and then affects the accuracy of the shockwave analysis [13][20].

2) The butterfly effect yielding backward shockwaves and unstable vehicle traffic flow are difficult to be addressed in a fully distributed VANET [17][18][22].

3) Most works only concern the average vehicle velocity, rather than concern some key parameters: traffic flow, traffic density, velocity variation [15][16][19][21].

The motivations of this paper aim to propose a platoon-based cooperative approach that consists of three phases to avoid backward shockwaves and to increase driving stability and safety. The significant contributions include: 1) to minimize the backward shockwaves and the butterfly effects problem in active safe driving, 2) to adopt an

1. R.-H. Huang is with the department of Computer Science and Information Engineering, National Chung-Cheng University, Taiwan, ROC.
2. B.-J. Chang and Y.-L. Tsai are with the department of Computer Science and Information Engineering, National Yunlin University of Science and Technology, Taiwan, ROC. (Corresponding author: B.-J Chang; e-mail: changb@yuntech.edu.tw; phone: +886-5-5342601*4511; fax: +886-5-5312170).
3. Y.-H. Liang is with the department of Multimedia Animation and Application, Nan Kai University of Technology, Taiwan, ROC.

978-1-5386-5862-8/17 $31.00 © 2017 IEEE
DOI 10.1109/SC2.2017.13

adaptive platoon synchronization domain to dynamically determine the velocity and the platoon length, 3) to increase the driving stability and to minimize the waste of gasoline, 4) to achieve active safety driving efficiently, 5) to increase the road utilization, etc. Note that in platoon-based CACC the platoon length is defined as the maximum length of a vehicle-group, i.e., the distance from the first vehicle-member to the last one.

The reminder of this paper is organized as follows. The network model is defined in Section II. Section III details the proposed Cooperative Adaptive Driving (CAD) approach. Numerical results of simulations are provided in Section IV. Conclusions are given in Section V.

II. NETWORK MODEL

A vehicular network is defined as a directed graph $G=(V,E)$ that consists of a set of mobile vehicles V and a set of wireless links E, as demonstrated in Fig. 1. Some vehicles equipped with the Cooperative Adaptive Driving system (CAD) are denoted as V_j^{CAD} (or V_j), where j represents the vehicle index, i.e., the red vehicles that install the CAD system, wireless network and offer various-type sensors to sense vehicle traffic or environmental objects (including V_j^{CAD} and $V_j^{Non-CAD}$). Conversely, some vehicles not equipped with CAD are denoted as $V_k^{Non-CAD}$, as shown as the blue vehicles that can be sensed by V^{CAD} but cannot communicate with any vehicles because of lacking the wireless interface.

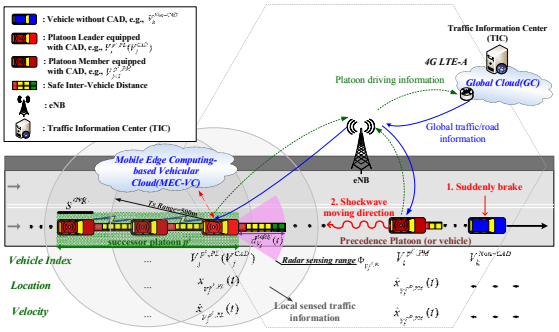

Fig. 1. Network Model

By using the wireless communications, two-types of clouds are formed: the global cloud (namely GC) and the vehicular cloud (VC)[26][27]. The CAD vehicles can receive the global traffic information from GC and receive the real-time-based local traffic information from VC managed by the platoon. The managed traffic information consists of the spatial and time localities-based information, such as the platoon identifier (PID), vehicle ID, geographical location, velocity, the limited speed of roads, etc.

The model considers a platoon-based mechanism, in which for any two adjacent platoons p^s denotes the successor platoon and p^p denotes the precedence platoon. The average velocity and the length of the platoon (e.g., p^s) at time t are denoted as $\bar{v}_{p^s}(t)$ and $L_{p^s}(t)$, respectively. $N_{p^s}(t)$ denotes the total number vehicles of platoon p at time t.

In a platoon p, it consists of two types of vehicles: the platoon leader (e.g., $V_j^{p^s,PL}$) and the platoon members. Thus, the geographical location and velocity of the platoon leader j at time t are denoted as $x_{V_j^{p^s,PL}}(t)$ and $\dot{x}_{V_j^{p^s,PL}}(t)$, respectively. Moreover, the distance to the ahead adjacent vehicle is sensed by the radar sensor and it is denoted as $\Phi_{V_j^{p^s,PL}}$. To guarantee safe driving, $\Phi_{V_j^{p^s,PL}}$ should be smaller than the determined safe inter-vehicle distance at time t, $d_{V_j}^{Safe}(t)$. $d_{V_j}^{Safe}(t)$ is dynamically determined according to three parameters: 1) the moving distance after a response at time t, denoted as $d_{V_j}^{Response}(t)$, 2) the required distance of a full stop at time t, denoted as $d_{V_j}^{Brake}(t)$, and 3) the distance for the transmission of synchronization message at time t, denoted as $d_{V_j}^{Sync.}(t)$. Furthermore, we assume that the minimum distance of the standstill vehicle is s^{bumper}.

Additionally, when the traffic flow (q_{p^p}) and the average vehicle velocity ($\bar{v}_{p^p}$) decrease and the vehicle density (k_{p^p}) increases of the precedence platoon, p^p, the successor platoon, p^s, easily yields a backward shockwave. The shockwave speed, $W_{p^{p-s}}^{V}$, can be determined by the differences of the traffic flow, the average vehicle velocity, and the vehicle density of the successor and the precedence platoons.

III. THE PROPOSED CAD APPROACH

This section details the proposed approach of Cooperative Adaptive Driving (CAD) that consists of two phases.

3.1 Phase 1: Cooperative Vehicle Platooning (CVP) phase

For minimizing the butterfly effect and shockwaves, CAD proposes an adaptive management for the cooperative vehicle platooning (CVP) driving as the key element for realizing CAD. Fig. 2 demonstrates that the vehicles of a platoon p^s exhibits two roles: 1) a platoon leader (e.g., $V_j^{p^s,PL}$) and 2) the platoon members (e.g., $V_{j+1}^{p^s,PM}$).

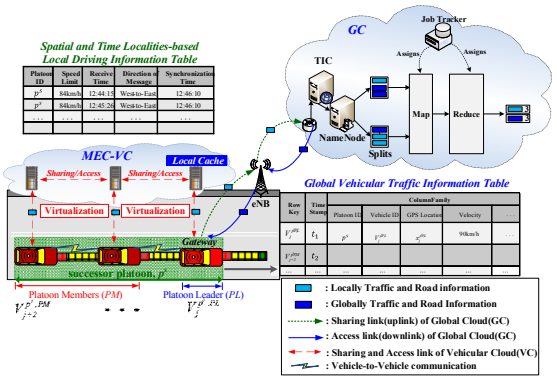

Fig. 2. Driving state of CAD approach

3.1.1. Platoon Leader (PL)

In CAD, for minimizing the minimize the computing and

transmission delay, the Mobile Edge Computing (MEC) mechanism [23]-[25] is adopt to move the computing-intensive and data-intensive virtual machine instances of the global cloud to the local site that is near to users. Furthermore, the MEC mechanism is combined and cooperated with the Vehicular Cloud (namely VC or MEC-VC) to achieve real-time computing, to minimize transmission delay, and to allocate/re-direct the optimal VM instances of diverse applications to the platoon.

Thus, in CAD, the first vehicle forming a platoon or the vehicle with the least MAC address will be selected as the Platoon Leader (PL) when the platoon is initialized. The PL acts as the centralized platoon header that manages the entire platoon synchronization and maintains the platoon traffic information of each platoon member in a local vehicle cloud (VC) table, as shown in Fig. 2 and detailed below.

First, PL manages the platoon members when some of them join to/leave from the platoon. Second, by using a local vehicle cloud, PL maintains the sensed/received traffic information that are gathered from the sharing broadcast messages sent by PMs. Note that the sharing message with timestamp are forwarded within a limited hop-count, i.e., the synchronization platoon length $L_{p^s}(t)$, determined by Phase 3. Third, PL determines the platoon velocity and the platoon synchronous length, and then broadcasts the up-to-date control message to all PMs periodically or on demand. Thus, the PMs can synchronously adjust their velocity at next synchronization time $\tau^{Sync.}_{V_j^{p^s},PL}$.

For timely keeping and updating the local real-time traffic information in the local MEC-VC, the Cooperation as a Service (CaaS) cloud computing mechanism is proposed herein and managed by PL, as demonstrated in Fig. 2. The local VC keeps the dynamic driving state of each PM, including 1) platoon ID, 2) vehicle ID, 3) GPS location, 4) vehicle velocity, 5) the highest velocity in history, 6) limited speed, 7) physical inter-distance, 8) logical inter-distance, 9) timestamp, 10) message ID, etc. Additionally, a global cloud (GC) is adopted for all vehicles of V^{CAD} located on different areas/roads sharing the traffic information, and thus the GC provides the global traffic and road information for every vehicle of V^{CAD}.

The main different functions between GC and VC are compared below. GC is a global-based Cloud Computing service that provides the global traffic/road information as completely as possible, but the global information may not be updated frequently. Conversely, VC is local-based Cloud Computing service that provides the local traffic/road information as fast as possible, but the local information may exclude the global information. Thus, by using the hybrid Cloud Computing services of MEC-VC and GC, the proposed cooperative platoon approach can offer both of the completely global information and the real-time local information.

Furthermore, PL determines the platoon velocity and the platoon synchronous length according to the traffic information. All PMs of the same platoon drive based on the received information. Note that the platoon length and velocity are determined adaptively. As a result, CAD can reduce asynchronous braking and avoid butterfly effects.

3.1.2. Platoon Member (PM)

In a platoon, a PM periodically sends beacon with its driving states to neighbors, and thus the PL can finally gather the driving information of all PMs within the platoon. The gathered driving information includes 1) Vehicle ID, 2) Geographical location, 3) Current Velocity, 4) Highest Velocity in History, 5) Physical Inter-distance, and 6) Receive time (Timestamp). Furthermore, PM adjusts the velocity and synchronization time after receiving the indication message sent from the PL.

Several platoon manage mechanisms are depicted as follows. First, when current PL leaves from the platoon, the PM located at the first one will be selected as the new PL because the PL of a platoon needs to lead the entire platoon moving forward. Second, when a vehicle with CAD moves alone, i.e., no neighbors around it, it initializes the PL selection procedure to select itself as the PL. Third, when two adjacent platoons move as closely as possible, the successor one will be merged into the precedence one.

3.2 Phase 2: Shockwave-Avoidance Driving (SAD) phase

In phase 1, the platoon is initialized and managed well. For avoiding shockwaves happened in the cooperative platoon-based driving, this section details SAD that consists of two sub-phases: 1) Maximum and Minimum Platoon Velocities and 2) Dynamic Safe Car-following Distance.

3.2.1 Phase2-1: Maximum and Minimum Platoon Velocities

In phase 2 (SAD), the main objective is to control the platoon moving stably safely. Two important factors affect the platoon stability: 1) a dynamic platoon velocity for all PMs of the platoon and 2) a dynamic platoon length for message synchronization. The determinations of these dynamic factors for a platoon are depicted in Phase 2-1 below.

In Fig. 3, in the case of non-platoon driving, a successive vehicle is affected by the precedent vehicle. Similarly, in the case of platoon driving, a successor platoon (p^s) is affected by the precedence platoon (p^p). Clearly, the shockwaves occurred between two platoons result from the inter-platoon operation. Thus, for the cooperative platoon driving, we first determine the traffic flow, traffic density and the average vehicle velocity of two adjacent platoons based on the traffic flow theory [28][29]. The traffic flow, q , is formulated as,

$$q(t) = k(t)\overline{v}(t), \tag{1}$$

where $k(t)$ is the traffic density at time t and $\overline{v}(t)$ is the average velocity at time t .The traffic density $k(t)$ can be formulated by $k(t) = \frac{N(t)}{L(t)}$, where $N(t)$ is the total number of vehicles on a road segment or within a platoon and $L(t)$ is the length of a road segment or the platoon length at time t . The speed of a shockwave can be determined by [28][29],

$$W^{V}_{p^{p-s}}(t) = \frac{q_{p^p}(t) - q_{p^s}(t)}{k_{p^p}(t) - k_{p^s}(t)}, \tag{2}$$

where the traffic flow of the successor and precedence platoons ($q_{p^s}(t)$ and $q_{p^p}(t)$) can be obtained by Eq. (1). The traffic density of the successor and precedence platoons at time t ($k_{p^s}(t)$ and $k_{p^p}(t)$) are the determined parameters. In consequence, a backward shockwave at time t , i.e., $W^V_{p^{p-s}}(t) < 0$, exhibits when the following conditions happen: 1) $q_{p^p}(t) < q_{p^s}(t)$, 2) $k_{p^p}(t) > k_{p^s}(t)$ and 3) $\bar{v}_{p^p}(t) < \bar{v}_{p^s}(t)$. Clearly, to avoid happening a shockwave, the speed of a shockwave should not be a negative value, i.e., $W^V_{p^{p-s}}(t) \geq 0$. We have,

$$W^V_{p^{p-s}}(t) = \frac{q_{p^p}(t) - q_{p^s}(t)}{k_{p^p}(t) - k_{p^s}(t)} = \frac{\frac{N_{p^p}(t)\bar{v}_{p^p}(t)}{L_{p^p}(t)} - \frac{N_{p^s}(t)\bar{v}_{p^s}(t)}{L_{p^s}(t)}}{\frac{N_{p^p}(t)}{L_{p^p}(t)} - \frac{N_{p^s}(t)}{L_{p^s}(t)}} > 1. \quad (3)$$

The maximum platoon velocity ($\bar{v}^{max}_{p^s}(t)$) at time t of the successor platoon (p^s) can be derived from Eq. (3),

$$\bar{v}^{max}_{p^s}(t) \leq -\left(\frac{N_{p^p}(t)L_{p^s}(t)\left(1-\bar{v}_{p^p}(t)\right)}{N_{p^s}(t)L_{p^p}(t)} - 1 \right). \quad (4)$$

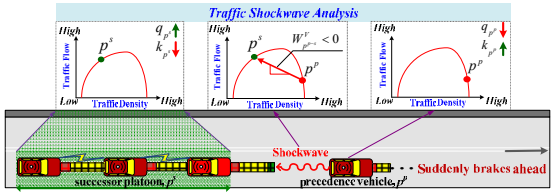

Fig. 3. Traffic Shockwave Analysis of CAD approach

Additionally, for increasing the driving efficiently, the minimum platoon velocity needs to be determined according to the local driving information and the history information, as indicated,

$$\bar{v}^{min}_{p^s}(t) \geq \min_{\forall N_{p^s}(t)} \{ \textit{The highest velocity in history} \}, \quad (5)$$

where $N_{p^s}(t)$ is the number of vehicle of the successor platoon (p^s) at time t .

3.2.2 Phase 2-2: Dynamic Safe Car-following Distance

For safe driving, a dynamic safe car-following distance is an important factor to be determined for every vehicle. A high speed vehicle needs a longer safe car-following distance, and vice versa. This paper proposes a dynamic safe car-following distance for the cooperative platoon driving, as detailed below.

In CAD, a platoon leader (PL) adopts the synchronization message to send the platoon synchronization time and to maximum platoon velocity to all PMs for minimizing the shockwaves and the butterfly effects. Before detailing Phase 2-2, the terms of the shockwave affection range ($W^R_{p^{p-s}}(t)$) and the synchronous message distance ($d^{Sync}_{V^{p,PL}_j}(t)$) should be introduced clearly. First, the (backward) shockwave can be detected by the PL ($x_{V^{p^s,PL}_j}(t)$) and the shockwave affection range ($W^R_{p^{p-s}}(t)$) can be estimated by the shockwave speed ($W^V_{p^{p-s}}(t)$) as shown in Eqs. (3)(9).

Second, the shockwave affection range ($W^R_{p^{p-s}}(t)$) will be adopted for the determination of the synchronous message distance, $d^{Sync}_{V^{p,PL}_j}(t)$, as shown in Case 3 of this section. Note that the synchronization length should be shorter than the shockwave affection range, i.e., $d^{Sync}_{V^{p,PL}_j}(t) < W^R_{p^{p-s}}(t)$.

As demonstrated in Fig. 4, in CAD, an adaptive safe extended car-following distance for PL, $V^{p,PL}_j$, at time t (namely $d^{Safe}_{V^{p,PL}_j}(t)$) is proposed to keep an absolute safe distance for the platoon. $d^{Safe}_{V^{p,PL}_j}(t)$ consists of three parts: 1) the moving distance of the response time to brake, denoted by $d^{Response}_{V^{p,PL}_j}(t)$, 2) the distance of the bake to full stop, $d^{Brake}_{V^{p,PL}_j}(t)$, 3) the distance required for the transmission of synchronous message from the precedence platoon that detects a shockwave, $d^{Sync}_{V^{p,PL}_j}(t)$ .That is,

$$d^{Safe}_{V^{p,PL}_j}(t) \leftarrow d^{Response}_{V^{p,PL}_j}(t) + d^{Brake}_{V^{p,PL}_j}(t) + d^{Sync.}_{V^{p,PL}_j}(t). \quad (6)$$

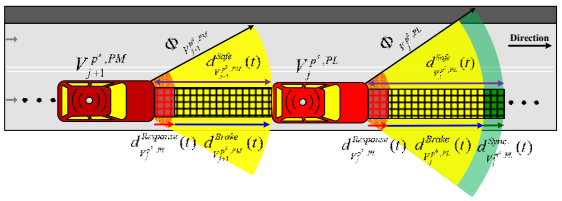

Fig. 4. The safe extended car-following distance of PL and PM in CAD

Case 1. The response distance, $d^{Response}_{V^{p,PL}_j}(t)$

A brake may be initialized by a driver or an assistant longitudinal control unit. During the response delay, a moving vehicle has been moved forward the distance of $d^{Response}_{V^{p,PL}_j}(t)$ before braking, as indicated,

$$d^{Response}_{V^{p,PL}_j}(t) = \beta \cdot \dot{x}_{V^{p,PL}_j}(t), \quad (7)$$

where β represents the response time and $\dot{x}_{V^{p,PL}_j}(t)$ represents the vehicle velocity at time t .

Case 2.The brake distance, $d^{Brake}_{V^{p,PL}_j}(t)$

Based on the Newton's laws of motion, the distance required for a moving vehicle to full stop with a deceleration $\dot{x}_{V^{p,PL}_j}(t)$ and the minimum distance of the standstill vehicle, s^{bumper} , can be determined by,

$$d^{Brake}_{V^{p,PL}_j}(t) = \frac{\dot{x}_{V^{p,PL}_j}(t)^2}{2 \cdot g \cdot \mu(t)} + s^{bumper}, \quad (8)$$

where g represents the gravitational acceleration, i.e., 9.8m/s^2, and $\mu(t)$ represents the coefficient of friction between the tire and road surface at time t [30]. Note that s^{bumper} is defined as 1/2 or one vehicle length. s^{bumper} is required even though the PL is at the moving state.

Case 3. The synchronous message distance, $d^{Sync}_{V_j^{p,PL}}(t)$

The objective of the determination of the synchronous message distance, $d^{Sync}_{V_j^{p,PL}}(t)$, is for the successor platoon to control the platoon velocity synchronously stably. Thus, the happened shockwave at precedence will not affect the driving of the successor platoons obviously. The transmission delay of the emergency message becomes important in CAD.

In CAD, a PL can detect a shockwave by two methods. First, the PL actively detects a shockwave resulted from the suddenly braking of the precedence vehicle. Second, a precedence platoon or vehicle detects there is a shockwave with a backward propagation speed (successor propagation), $W^V_{p^{p-s}}(t)$, and then the precedence platoon sends an emergency message with the traffic flow and the traffic density of the precedence, $q_{p^p}(t)$ and $k_{p^p}(t)$, to notify the successor platoons or vehicles, i.e., the PL. Then, by using the traffic analysis in Eq. (2), we can obtain the shockwave moves from the precedence platoon to the successor platoon with the speed of $W^V_{p^{p-s}}(t)$. Thus, the affected range of the shockwave at time t, denoted by $W^R_{p^{p-s}}(t)$, can be determined by the shockwave speed ($W^V_{p^{p-s}}(t)$) and the "time headway" that is the elapsed time between the time that one vehicle finishes passing a fixed observation point and the instant that the next vehicle starts to pass that point, as indicated,

$$W^R_{p^{p-s}}(t) = W^V_{p^{p-s}}(t) \cdot \frac{x_{V_i^{p^p,PM}}(t) - x_{V_j^{p^s,PL}}(t) - s^{avg.}}{\dot{x}_{V_j^{p^s,PL}}(t)}. \quad (9)$$

In Eq. 9, $x_{V_i^{p^p,PM}}(t)$ and $x_{V_j^{p^s,PL}}(t)$ represent the geographical locations of vehicles $V_i^{p^p,PM}$ and $V_j^{p^s,PL}$ at time t, respectively, $\dot{x}_{V_j^{p^s,PL}}(t)$ denotes the velocity of vehicle $V_j^{p^s,PL}$ at time t, and $s^{avg.}$ denotes the average vehicle length.

After obtaining the shockwave affection range, the time required for the emergency message transmission from the vehicle detecting the shockwave to the successor platoon can be computed by the hop-to-hop transmission delay (D_{h2h}), as indicated,

$$D_{h2h} = \left(D_{access} + D_{trans.}\right) \cdot \left\lceil \frac{W^R_{p^{p-s}}(t)}{T_x^{range}} \right\rceil, \quad (10)$$

where T_x^{range} is the wireless transmission range, $\left\lceil \frac{W^R_{p^{p-s}}(t)}{T_x^{range}} \right\rceil$ is the number of hops and the transmission time of a single wireless hop at time t consisting of two parts: $\left(D_{access} + D_{trans.}\right)$. Note that in the single hop transmission time, we only consider the access delay D_{access} and the packet transmission delay $D_{trans.}$, but neglects the queueing delay D_{queue}, propagation delay $D_{propagation}$ and the processing delay $D_{processing}$ because of too small.

The access delay D_{access} and the packet transmission delay $D_{trans.}$ are determined as follows. First, for D_{access}, we assume that CAD's VANET adopts IEEE 802.11p with the Enhanced Distributed Channel Access as the wireless interface. EDCA uses CSMA/CA as the channel contention access mechanism. We assume that a packet before successful transmission exhibits an average number of contentions (including the first transmission and the other number of re-transmissions), as denoted by $\gamma^{avg.}$. In a contention, the contention delay consists of the AIFS period and the backoff-time. As a result, the access delay D_{access} can be formulated by [31],

$$\begin{aligned} D_{access} &= \gamma^{avg.} \cdot \left(Backoff\ Time + AIFS\right) \\ &= \gamma^{avg.} \cdot \left[(Random() \cdot \tau_{slot}) + (AIFSN \cdot \tau_{slot} + 2 \cdot \tau_{slot}) \right] \\ &= \gamma^{avg.} \cdot \left[\tau_{slot} (Random() + AIFSN + 2) \right]. \end{aligned} \quad (11)$$

where $Random()$ denotes the randomly waiting delay and $\gamma^{avg.} = p_c^{avg.} \gamma^{max}$. $p_c^{avg.}$ is the average collision probability and γ^{max} is the maximum retry limit. Moreover, $AIFSN$ uses two slots. Note that 1 slot time is $16\mu s$ in IEEE 802.11p [32].

Second, for $D_{trans.}$, it can be determined by $D_{trans.} = \frac{l}{T_x^{rate}}$, where l means the packet length in bit and T_x^{rate} means the wireless transmission rate.

Finally, the PL of the successor platoon moves the distance required for the transmission of synchronous message from the precedence vehicle or platoon by

$$d^{Sync.}_{V_j^{p^s,PL}}(t) = D_{h2h} \cdot \dot{x}_{V_j^{p^s,PL}}(t). \quad (12)$$

Note that, in the analysis, the average collision probability, $p_c^{avg.}$, is randomly determined. That is, the access delay and the transmission delay have been considered, and the connectivity of packet transmission is considered. Clearly, the hop-to-hop transmission delay is not a fixed robust one.

In Fig. 5, the idea of APS is to synchronize the velocity change of each PM within platoon p. Three key factors: **1)** determining the dynamic platoon length according to the hop delay, **2)** computing the next synchronization time and **3)** synchronizing the platoon velocity, should be solved for achieving APS successfully.

First, the message transmission time is limited according to the driving time for the PL ($V_j^{p,PL}$) with velocity of $\dot{x}_{V_j^{p,PL}}(t)$, as

$$\left(D_{access} + D_{trans.}\right) \left\lceil \frac{L_p(t+1)}{T_x^{range}} \right\rceil \le \frac{d^{Sync.}_{V_j^{p,PL}}(t)}{\dot{x}_{V_j^{p,PL}}(t)}, \quad (13)$$

where $L_p(t+1)$ means the platoon length at time t and $(D_{access}+D_{trans.})$ denotes one hop delay. As a result, the platoon length $L_p(t+1)$,

$$L_p(t+1) \le \frac{d^{Sync.}_{V_j^{p,PL}}(t)\cdot T_x^{range}}{\dot{x}_{V_j^{p,PL}}(t)\cdot(D_{access}+D_{trans.})}. \quad (14)$$

Second, after obtaining the platoon length, the synchronization for next time for PMs of platoon p, denoted by $\tau^{Sync.}_{V_j^{p,PL}}$, can be determined by PL,

$$\tau^{Sync.}_{V_j^{p,PL}} = T_{curr} + \frac{d^{Sync.}_{V_j^{p,PL}}(t)}{\dot{x}_{V_j^{p,PL}}(t)}, \quad (15)$$

where T_{curr} is current time when the platoon control message is sent. Note that the synchronization information sent by the platoon leader include: 1) the platoon ID, 2) the PL ID and position, 3) synchronization time ($\tau^{Sync.}_{V_j^{p,PL}}$.), and 4) limited speed ($\bar{v}_p^{max}(\tau^{Sync.}_{V_j^{p,PL}})$). Note that the synchronization length should be shorter than the shockwave affection range.

Finally, the adaptive platoon velocity for V_j at next synchronization time $\tau^{Sync.}_{V_j^{p,PL}}$, $\dot{x}_{V_j}(\tau^{Sync.}_{V_j^{p,PL}})$, can be obtained as follows,

$$\dot{x}_{V_j}(\tau^{Sync.}_{V_j^{p,PL}}) = \dot{x}_{V_j}(t) + a_{V_j}\cdot\Delta t, \quad (16)$$

where Δt represents the time interval of synchronization.

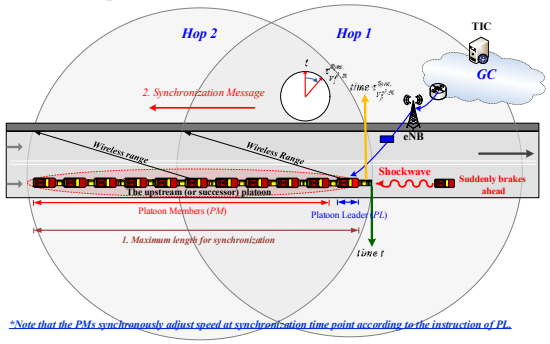

Fig. 5. The adaptive platoon synchronization in CAD

IV. Numerical Results

In this section, the proposed *CAD* approach is evaluated by comparing with several important approaches: the Integrated full-Range Speed Assistance (namely *IRSA*) [20], Intelligent Driver Model (namely *IDM*) [33], and Human driving (namely *HUMAN*). *IRSA* models the driving behavior extended from the CACC and *IRSA* determines the driving velocity according to the average velocity of three precedence vehicles. *IDM* models the driving behavior extended from the ACC and considers the 1.5 sec time headway. In the *HUMAN* driving model, we consider some parameters: 1) delayed response time, 2) random response time (1~2 seconds) for determining the car-following distance, etc. to simulate driving behaviors by [34].

The evaluated network model is a two-lane one-kilometer long road, in which the average vehicle length is set to 6 meters and the minimum distance of the standstill vehicle is set to 3 meters. In the traffic model, the incoming vehicles initiated at the start-end point is generated by the Poisson distribution with arrival rate λ [35] and the inter-vehicle distance is formulated by the IDM with continuous function [33]. The vehicle mobility model is generated by the Normal distribution with average velocity μ and variance σ^2 [36], where the average velocity of evaluations are generated between 80 and 110 km/hr.

Figs. 6(a)-(c) demonstrate the velocity joint position trajectory results affected by shockwaves among all compared approaches (*CAD, ISRA,* and *HUMAN*), in which the suddenly braking events happen at the 60-th second.

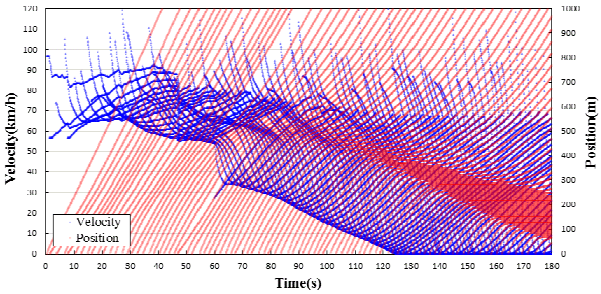

Fig. 6(a). The velocity joint position trajectory of *HUMAN*

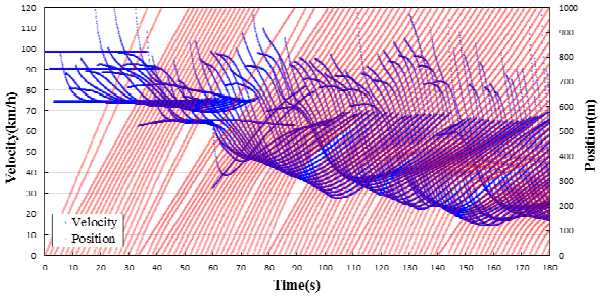

Fig. 6(b). The velocity joint position trajectory of *IRSA*

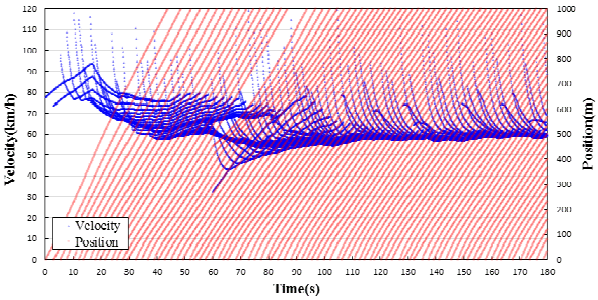

Fig. 6(c). The velocity joint position trajectory of *CAD*

In Fig. 6(a), in the case of *HUMAN*, the suddenly braking results in all vehicles decreasing their velocities during t=60~125 (sec). Moreover, the event leads to the butterfly effect that decreases the velocity of all affected vehicles to 0 km/h during t=125~180 (sec). In Fig. 6(b), in the case of *IRSA*, a vehicle refers to the velocities of (at most) three adjacent leading vehicles. The following vehicles thus can decrease their velocity in prior. The velocities of all vehicles are all above 14 km/h. However, without cooperation, the velocities of the following vehicles change inconsistently, and then results in unstable driving. In Fig. 6(c), *CAD* adopts the cooperative platoon-based control. The velocities of the

following vehicles change consistently based on, even though it exhibits a suddenly braking at t=60 (sec) and only affects a consistent velocity decreasing during t=60~70(sec). Then, the following vehicles restore the velocities up to 70 km/h. That is, *CAD* can effectively avoid the butterfly effects resulted from a suddenly braking.

Figs. 7(a)-(b) show the 3D of the velocity joint position trajectory results of *ISRA* and *CAD*, in which the suddenly braking events happen every interval of 60-second. In Fig. 7(a), *ISRA* yields obvious velocity changes, as shown in the red area, while exhibiting sudden brakes. IRSA suffers from asynchronously change the velocities of neighbor vehicles, and then significantly decreases the velocity while exhibiting shockwaves. In Fig. 7(b), *CAD* outperforms *ISRA* in the avoidance of butterflies, so the 3D trajectory of *CAD* is changed smoothly. The reason is the platoon-based *CAD* adaptively determines the platoon velocity and the safe distance for platoon synchronization.

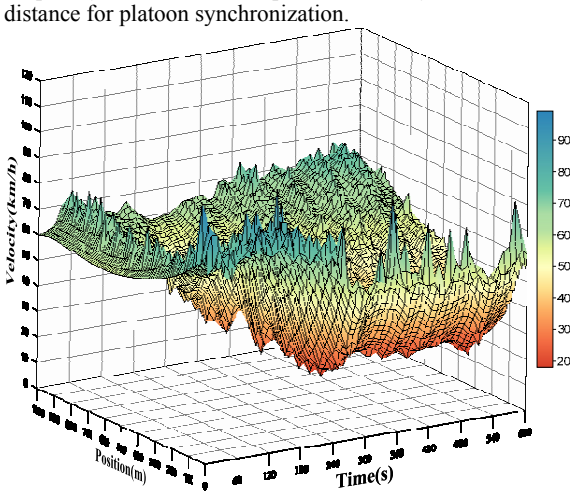

Fig. 7(a). 3D velocity joint position trajectory of *IRSA*

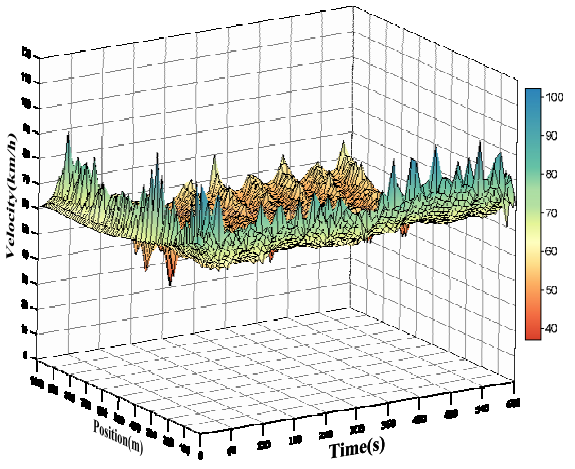

Fig. 7(b). 3D velocity joint position trajectory of *CAD*

Fig. 8 compares the number of shockwaves under different traffic loads ranging from 1 to 5 Erlangs. *CAD* yields none shockwave, but *HUMAN* yields the highest number of shockwaves. Furthermore, *IRSA* yields a fewer number of shockwaves than that of *IDM*. Moreover, the number of shockwaves of all compared approaches (except *CAD*) increase as traffic load increasing.

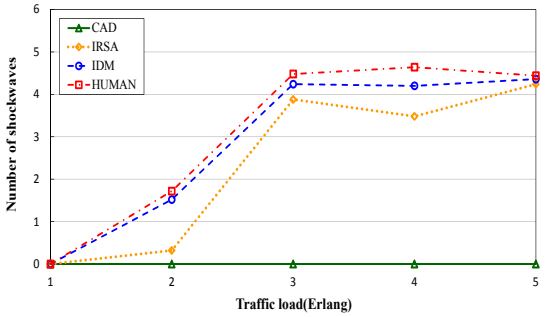

Fig. 8. Number of shockwaves under different traffic loads

Fig. 9 compares the average vehicle velocities of all compared approaches under different traffic loads ranging from 1 to 5 Erlangs. The velocities of all approaches decrease as traffic load as increasing. *CAD* yields a higher velocity, but *HUAMN* and *IDM* yield a lower velocity. The reason is that *CAD* exhibits a stable velocity by using the cooperative platoon-based driving, so the vehicles synchronously change their velocities. However, *HUMAN* and *IDM* lack the cooperative CACC mechanism, the vehicle velocity is changed inconsistently, and results in unstable velocity and a lower average velocity.

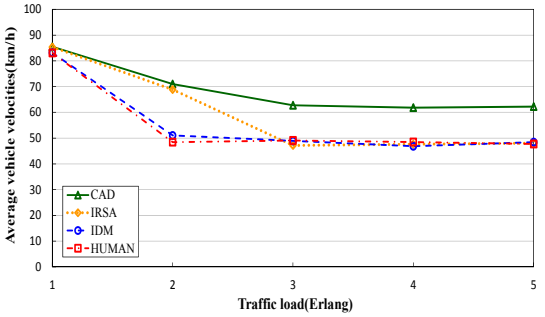

Fig. 9. Average vehicle velocities under different traffic loads

V. CONCLUSIONS

Intelligent Transportation System aims to achieve safe driving actively, less travel time, stable vehicle velocity, etc. Without using the cooperative-based active safe driving, above mentioned objectives are difficult to be fulfilled. However, the Cooperative active safe driving mechanism suffers from the suddenly braking that easily leads to butterfly effects and brings several challenges: shockwaves, unstable driving, unsafe driving, long travel time, etc. Thus, this paper proposed the Mobile Edge Computing-based CAD approach to minimize butterfly effects and shockwaves, and then achieves active safe driving. The main contributions of CAD include: 1) adaptively determining the platoon velocity according to the traffic information, 2) determining the safe distance for platoon synchronization, 3) adaptively determining the platoon length, 4) avoiding butterfly effects and shockwaves, etc. Numerical results demonstrate CAD outperforms the compared approaches in the number of shockwaves, and average velocity. In addition, CAD achieves to determine the adaptive platoon length according to traffic information gathered from the global and local clouds.

ACKNOWLEDGEMENTS

This research was supported in parts by the Ministry of Science and Technology of Taiwan, ROC, under Grants MOST106-2221-E-194-021-MY3,MOST-105-2221-E-224-031-MY2, MOST-106-2511-S-252-001, and MOST-106-3011-F-252-001.

REFERENCES

[1] M. Burke and J. Williams, "Cooperative ITS Regulatory Policy Issues: Discussion Paper," Australia National Transport Commission, Nov. 2012.

[2] Intelligent Transportation Systems (ITS), http://www.its.dot.gov/

[3] IEEE Std. for Information technology-Telecommunication and information exchange between systems-Local and metropolitan area networks-Specific requirements, IEEE Std. 802.11p, Jul. 2010.

[4] IEEE Trial-Use Standard for Wireless Access in Vehicular Environments (WAVE)—Multi-channel Operation, IEEE Std. P1609.4, Nov. 2006.

[5] RP-161894, "LTE-based V2X Services", 3GPP, Sep. 2016.

[6] Shanzhi Chen, Jinling Hu, Yan Shi, and Li Zhao, "LTE-V: A TD-LTE-Based V2X Solution for Future Vehicular Network," *IEEE Internet of Things Journal*, Vol. 3, No. 6, pp. 997-1005 Dec. 2016.

[7] C. Maag, D. Mühlbacher, C. Mark and H.-P. Krüger, "Studying Effects of Advanced Driver Assistance Systems (ADAS) on Individual and Group Level Using Multi-Driver Simulation," *IEEE Intelligent Transportation Systems Magazine*, Vol. 4, No. 3, pp. 45–54, Fall 2012.

[8] J.Pauwelussen and P. J. Feenstra, "Driver Behavior Analysis during ACC Activation and Deactivation in a Real Traffic Environment," *IEEE Trans. on Intelligent Transportation Systems*, Vol. 11, No. 2, pp. 329–338, Jun. 2010.

[9] R. Stevenson, "A Driver's Sixth Sense," *IEEE Spectrum*, Vol. 48, No. 10, pp. 50–55, Oct. 2011.

[10] P. Papadimitratos, A. La Fortelle, K. Evenssen, R. Brignolo and S. Cosenza, "Vehicular Communication Systems: Enabling Technologies, Applications, and Future Outlook on Intelligent Transportation," *IEEE Comm. Magazine*, Vol. 47, No. 11, pp. 84 – 95, Nov. 2009.

[11] C. Desjardinsand and B. Chaib-draa, "Cooperative Adaptive Cruise Control : A Reinforcement Learning Approach," *IEEE Trans. on Intelligent Transportation Systems*, Vol. 12, No. 4, pp. 1248–1260, Dec. 2011.

[12] E. Lorenz, "Deterministic Nonperiodic Flow," *Journal of the Atmospheric Sciences*, Vol. 20, No. 2, pp. 130–141, Mar. 1963.

[13] G. K. Mitropoulos, I. S. Karanasiou, A. Hinsberger, F. Aguado-Agelet, H. Wieker, H.-J. Hilt, S. MammarandG. Noecker, "Wireless Local Danger Warning: Cooperative Foresighted Driving Using Intervehicle Communication," *IEEE Trans. on Intelligent Transportation Systems*, Vol. 11, No.3, pp. 539–553, Sep. 2010.

[14] C.-L. Huang, Y.P. Fallah, R. Sengupta and H. Krishnan, "Adaptive Intervehicle Communication Control for Cooperative Safety Systems," *IEEE Network*, Vol. 24, No. 1, pp. 6–13, Jan.-Feb. 2010.

[15] T. Taleb, A. Benslimane and K.B. Letaief, "Toward an Effective Risk-Conscious and Collaborative Vehicular Collision Avoidance System," *IEEE Trans. on Vehicular Technology*, Vol. 59, No.3, pp. 1474–1486, Mar. 2010.

[16] V. Milanés, J. Alonso, L. Bouraouiand J. Ploeg, "Cooperative Maneuvering in Close Environments Among Cybercars and Dual-Mode Cars," *IEEE Trans. on Intelligent Transportation Systems*, Vol. 12, No. 1, pp. 15–24, Mar. 2011.

[17] V. Milanés, J. Godoy, J. Villagra and J. Perez, "Automated On-Ramp Merging System for Congested Traffic Situations," *IEEE Trans. on Intelligent Transportation Systems*, Vol. 12, No. 2, pp. 500–508, Jun. 2011.

[18] N. Geroliminis and A. Skabardonis, "Identification and Analysis of Queue Spillovers in City Street Networks," *IEEE Trans. on Intelligent Transportation Systems*, Vol. 12, pp. 1107–1115, No. 3, Dec. 2011.

[19] W.J. Schakel, B. v. Arem and B.D. Netten, "Effects of Cooperative Adaptive Cruise Control on Traffic Flow Stability," *2010 IEEE Conference on Intelligent Transportation Systems (ITSC)*, pp. 759–764, Sep. 2010.

[20] I.R. Wilmink, G. A. Klunder and B.v. Arem, "Traffic Flow Effects of Integrated Full-Range Velocity Assistance (IRSA)," *2007 IEEE Intelligent Vehicles Symposium*, pp. 1204–1210, Jun. 2007.

[21] F.H. Somda and H. Cormerais, "Auto-Adaptive and String Stable Strategy for Intelligent Cruise Control," *IET Intelligent Transport Systems*, Vol. 5, No. 3, pp. 168–174, Sep. 2011.

[22] B. Asadi and A. Vahidi, "Predictive Cruise Control: Utilizing Upcoming Traffic Signal Information for Improving Fuel Economy and Reducing Trip Time," *IEEE Trans. on Control Systems Technology*, Vol. 19, No. 3, pp. 707–714, May 2011.

[23] A. S. Gomes, B. Sousa, D. Palma, V. Fonseca, Z. Zhao, E. Monteiro, T. Braun, P. Simoes and L. Cordeiro, "Edge caching with mobility prediction in virtualized LTE mobile networks," *Future Generation Computer Systems*, Vol. 70, pp. 148-162, May 2017.

[24] T. Q. Dinh, J. Tang, Q. D. La and T. Q. S. Quek, "Offloading in Mobile Edge Computing: Task Allocation and Computational Frequency Scaling," *IEEE Trans. on Communications*, Vol. 99, 2017. (10.1109/TCOMM.2017.2699660)

[25] D. Satria, D. Park and M. Jo, "Recovery for overloaded mobile edge computing," *Future Generation Computer Systems*, Vol. 70, pp. 138-147, May 2017.

[26] M. Abuelela and S. Olariu, "Taking VANET to the Clouds," *International Conference on Advances in Mobile Computing and Multimedia*, pp. 6–13, Nov. 2010.

[27] H. Mousannif, I. Khalil and H. A. Moatassime, "Cooperation as a Service in VANETs," *Journal of Universal Computer Science,* Vol. 17, No. 8, 2011.

[28] R. Kuhne and P. Michalopoulos, "CONTINUUM FLOW MODELS," Transportation Research Board (TRB) Special Report 165, 1992.

[29] D. Helbing, "Traffic and related self-driven many-particle systems," *Reviews of Modern Physics*, Vol. 73, No. 4, pp. 1067–1141, Oct. 2001.

[30] Ministry of Transportation and Communications (MOTC), http://www.iot.gov.tw

[31] Part 11: Wireless LAN Medium Access Control (MAC) and Physical Layer (PHY) Specifications Amendment: Medium Access Control (MAC) Quality of Service Enhancements, *IEEE Std. 802.11e*, Nov. 2005.

[32] S. Öztürk and J. Mišić, "On non-saturation regime in IEEE 802.11p based VANET with mobile nodes," *IEEE PIMRC 2011*, pp. 740–744, Sep. 2011.

[33] M. Treiber, A. Hennecke and D. Helbing, "Congested Traffic States in Empirical Observations and Microscopic Simulations," Physical Review E62, pp. 1805–1824, Aug. 2000.

[34] Microsimulation of Road Traffic Flow, http://www.traffic-simulation.de/

[35] W. J. Thompson, "Poisson distributions," *Computing in Science & Engineering*, Vol. 3, No. 3, pp. 78–82, May/June 2001.

[36] J. Tacq, "The Normal Distribution and its Applications," *International Encyclopedia of Education*, pp. 467–473, 2010.